Journal of Magnetic Resonance 196 (2009) 170–177

Contents lists available at ScienceDirect

Journal of Magnetic Resonance

journal homepage: www.elsevier.com/locate/jmr

Detection of glutamate and glutamine (Glx) by turbo spectroscopic imaging

Atiyah Yahya *, B. Gino Fallone

Department of Medical Physics, Cross Cancer Institute, 11560 University Avenue, Edmonton, Alta., Canada T6G 1Z2
Department of Oncology, University of Alberta, 11560 University Avenue, Edmonton, Alta., Canada T6G 1Z2

ARTICLE INFO

Article history:
Received 8 July 2008
Revised 14 October 2008
Available online 24 November 2008

Keywords:
Turbo spectroscopic imaging
RF pulse bandwidth
Chemical shift displacement
Glutamate
Brain

ABSTRACT

Turbo spectroscopic imaging (TSI) is a spin echo spectroscopic imaging technique in which two or more echoes are acquired per excitation to reduce the acquisition time. The application of TSI has primarily been limited to the detection of uncoupled spins because the signal from coupled spins is modulated as a function of echo time. In this work we demonstrate how the TSI sequence can be modified to observe spins like the C_2 protons of Glx (≈3.75 ppm) which are involved solely in weak-coupling interactions. The technique exploits the chemical shift displacement effect by employing TSI refocusing pulses that have bandwidths which are less than the chemical shift difference between the target spins and the spins to which they are weakly coupled. The modified TSI sequence rewinds the *J*-evolution of the target protons in the slice of interest independently of the echo time or echo spacing, thereby removing any signal variation between successive echoes (apart from T_2 relaxation effects). In this study we tailored the narrow-bandwidth TSI sequence for observation of the C_2 Glx protons. The echo time was experimentally optimized to minimize signal contamination from myo-inositol, and the efficacy of the method was verified on phantom solutions of Glx and on brain *in vivo*.

1. Introduction

Changes in the collective levels of glutamate (Glu) and glutamine (Gln), often referred to as Glx, have been shown to be relevant in the study of tumours as well as neurodegenerative and psychiatric diseases by proton magnetic resonance spectroscopy (MRS) investigations of the human brain [1–6]. While single voxel spectroscopy techniques are often employed for such studies, magnetic resonance spectroscopic imaging (MRSI) methods are becoming increasingly used as a result of recent technological advancements. Glx studies have been conducted using short echo time (TE) STimulated Echo Acquisition Mode [7], STEAM, or Point RESolved Spectroscopy [8], PRESS, MRSI sequences [5,9–11], where the volume of interest is excited via three orthogonal slice-selective pulses. The spin echo MRSI sequence [12] has also been employed to measure Glx levels [13]; it involves exciting an entire axial slice with a spin echo spectroscopic imaging sequence and using outer volume suppression (OVS) modules to suppress undesired signal from scalp lipids [12,14]. A significant advantage of the spin echo MRSI technique is that signal can be acquired from multiple slices without any scan time penalty [12,14]. For non-coupled spins, the acquisition time can be further reduced by acquiring more than one echo after each excitation pulse with each echo having a different phase encode gradient [15]. The multi-echo MRSI sequence, often referred to as Turbo Spectroscopic Imaging (TSI), allows faster acquisition times at the expense of spectral resolution because of the limited time available for signal readout between successive refocusing pulses [14]. Nevertheless, it was recently shown that at the higher clinical field strength of 3 T a spectral resolution of 8.8 Hz was sufficient to clearly resolve the creatine (Cr) and choline (Cho) peaks which are separated by approximately 0.16 ppm [16]. Ref. [16] also demonstrated that significant scan time reductions can be further made by combining TSI with SENSE (sensitivity encoding). While the clinical utility of TSI has been demonstrated for the detection of uncoupled spins such as those of *N*-acetyl aspartate (NAA), Cr, and Cho [16–19], its application to coupled spin systems is challenging because the scalar coupling evolution results in signal intensity and phase variations as a function of TE which can lead to spatial misregistration [20]. Moreover, for strongly coupled spins, such as the C_4 and C_3 protons of Glx, the signal rapidly decays with increasing TE rendering the long echo spacings (at least 100 ms) of TSI impractical for their detection.

In this work we present how the TSI sequence can be modified to allow the detection of spins such as the C_2 protons of Glx which are only involved in weak-coupling interactions. The technique is based on exploiting the chemical shift displacement effect so that the scalar coupling evolution of the C_2 Glx protons is "rewound" no matter what the echo time is, essentially removing any signal amplitude and phase variations with TE that would hinder the application of TSI. We recently demonstrated the theory behind

* Corresponding author. Address: Department of Medical Physics, Cross Cancer Institute, 11560 University Avenue, Edmonton, Alta., Canada T6G 1Z2.
E-mail address: ayahya@ualberta.ca (A. Yahya).

1090-7807/$ - see front matter © 2008 Elsevier Inc. All rights reserved.
doi:10.1016/j.jmr.2008.11.007

this concept and applied it to PRESS to obtain high signal from the C_2 protons of Glx at a long TE that enabled Glx levels to be quantified relative to Cr in a straightforward manner [21]. The method involved employing PRESS radiofrequency (RF) refocusing pulses that had bandwidths smaller than the chemical shift difference between the C_2 protons of Glx and the C_3 protons to which they are weakly coupled [21]. The objective of this paper is to show that the same method can be used to allow the efficient detection of the C_2 protons of Glx by a TSI sequence which reads out two echoes per excitation. The TE was optimized to minimize Glx signal contamination from myo-inositol (mI) and the efficacy of our method was verified at 3 T on phantom solutions of Glu and Gln and in brain *in vivo*.

2. Materials and methods

Glutamate and glutamine can each be represented, at 3 T, as an *AMNPQ* spin system where the *A* spin (bonded to the C_2 carbon) is weakly coupled to the *M* and *N* protons (both bonded to the C_3 carbon). The *M* and *N* protons are each strongly coupled to each other as well as to the *P* and *Q* protons (bonded to the C_4 carbon). To calculate the response of the *A* proton of Glu and of Gln at 3 T to a spin echo sequence as a function of TE the same numerical method described in Ref. [21] was employed.

Experiments were conducted with a 3 T Philips Intera scanner and a transmit/receive birdcage head coil. For all spectroscopic imaging experiments a two dimensional spin echo MRSI sequence, consisting of an excitation pulse and a refocusing pulse, both of which excited the same slice, was used. For TSI experiments, an additional refocusing pulse was applied, and two echoes were collected per excitation reducing the scan time by a factor of two; we chose to limit the number of echoes to two to minimize signal losses due to T_2 relaxation. Two versions of the sequence were employed. In one version, the refocusing pulses were sinc pulses of 870 Hz bandwidth and ≈10.3 ms duration. In the second version, the refocusing pulses were sinc Gaussian pulses of the same duration but with a narrow-bandwidth of 175 Hz which is less than the chemical shift difference between the C_2 and the C_3 protons of Glu and of Gln at 3 T (≈207 Hz). Spoiler gradients of length 2.5 ms and strength 10 mT/m were applied prior to and after the refocusing pulses in three orthogonal directions. All MRSI data was acquired as 256 complex points sampled at a frequency of 2000 Hz, yielding a spectral resolution of ≈7.8 Hz. The FID acquisition period was not centred symmetrically about the echo time but rather acquisition was initiated as soon as possible after the refocusing pulse was applied resulting in a minimum achievable TE of 100 ms for the TSI sequence. To obtain maximum signal from the C_2 protons of Glx from the slice of interest, the offset frequency of the pulses was set to approximately 3.75 ppm. A slice thickness of 15 mm was chosen for both phantom and *in-vivo* experiments. For phantoms, signal was collected over a field of view (FOV) of 80 mm with an 8×8 phase encode matrix, resulting in a nominal voxel size of $10 \times 10 \times 15$ mm^3, whereas for *in-vivo* studies signal was collected over a FOV of 240 mm with a 20×20 phase encode matrix yielding a nominal voxel size of $12 \times 12 \times 15$ mm^3. To minimize signal loss due to T_2 relaxation in the TSI data, signal from the first echoes filled the inner regions of *k*-space while signal from the second echoes filled the outer regions. The highest spatial frequencies located in the corners of *k*-space were not collected to reduce scan times. A repetition time (TR) of 3 s was employed in all the experiments resulting in a clinically acceptable acquisition time of approximately 8.5 min. Shimming was performed by a Philips-provided automatic procedure based on FASTERMAP [22] on a smaller volume ($80 \times 80 \times 15$ mm^3) which enclosed the region of interest within the FOV, and *in-vivo* water peak line widths were measured to be approximately 10 Hz. An outer volume suppression (OVS) module, which involved the excitation and dephasing of signal from ten 10 mm slabs placed around the volume of interest and over the skull regions, preceded the sequence. Prior to the OVS pulses, water suppression was carried out by a CHESS module [23] composed of 110 Hz bandwidth pulses. By gradually moving the offset frequencies of the CHESS pulses away from the water resonance frequency and measuring the amplitude of resulting the water peak, it was experimentally verified that the CHESS pulses had negligible effect on spins resonating at frequencies that deviated by more than 95 Hz from the frequency at which the pulses were applied safely excluding the C_2 Glx protons at about 3.75 ppm and the creatine (Cr) peak at 3.9 ppm. To prevent frequency drift effects, a frequency lock parameter was switched on which enabled the water resonance frequency to be measured and set for each acquisition. In an effort to assess the ability to quantify Glx levels from the TSI spectra, a short-TE (35 ms) PRESS single voxel spectrum was acquired in addition to the TSI spectra from two of the volunteers. The spatial location of the PRESS volume was chosen such that it overlapped with two of the TSI voxel

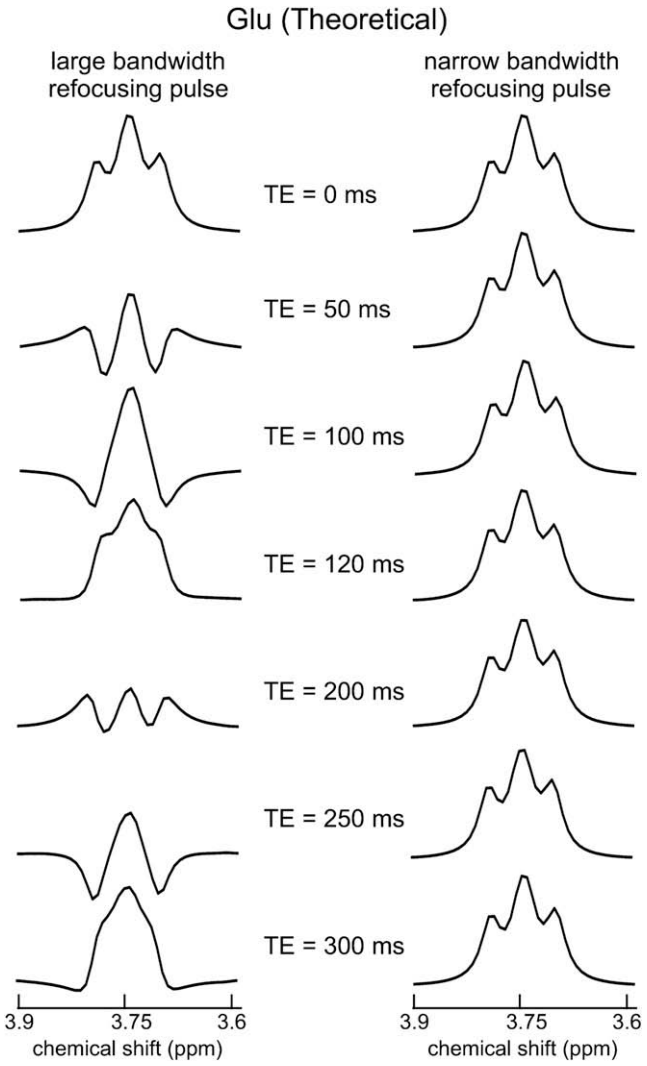

Fig. 1. The left-hand column displays the calculated response of the C_2 proton of Glu to a spin echo sequence which has a refocusing pulse that uniformly excites all the Glu protons. The signal is clearly modulated as a function of TE because of the weak scalar coupling interaction between the C_2 and C_3 Glu protons. In contrast, exploiting a refocusing pulse that exclusively targets the C_2 proton results in a triplet that remains practically unaltered as TE is changed, as shown on the right.

elements covering a $24 \times 12 \times 15$ mm^3 region. A TR of 3 s was used and the data was collected in 64 averages as 2048 complex points sampled at 2500 Hz.

Phantom experiments were conducted on four different 6 cm diameter spherical phantom solutions of pH $\approx$ 7. All of the phantoms contained 10 mM Cr and all chemicals were purchased from Sigma–Aldrich Canada. Three of the phantoms were composed of only one other component, namely, 50 mM Glu, 50 mM Gln, and 50 mM mI. The other phantom was composed of a mixture based on physiological concentration ratios present in gray matter of the human brain [24]; it contained 50 mM Glu, 24 mM Gln, and 31 mM mI.

Since the first echoes are responsible for filling the lower spatial frequencies and thus contribute most of the signal, an optimum TE for the small-bandwidth TSI sequence that minimized Glx contamination from mI was found by obtaining eleven data sets from the

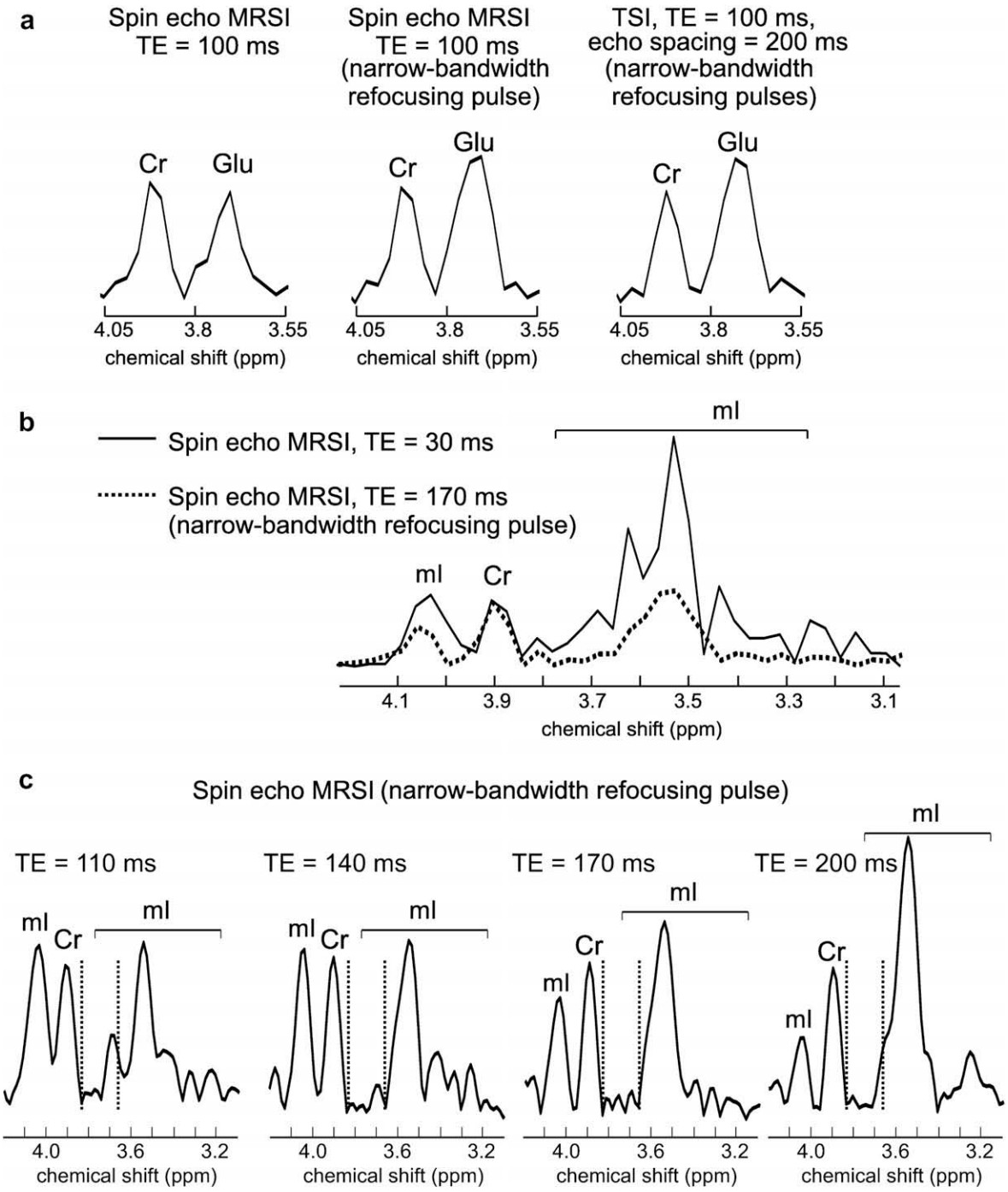

Fig. 2. All spectra in this figure are from a central voxel of the MRSI acquisition grid, and are displayed in magnitude mode. Panel (a) shows spectra acquired from the 50 mM Glu/10 mM Cr phantom. The amplitude of the Glu peak increases by approximately 30% when replacing the 870 Hz bandwidth refocusing pulse with one that has a bandwidth of 175 Hz. Applying a TSI sequence where two echoes per excitation are acquired (employing two narrow-bandwidth refocusing pulses) does not appear to affect the quality of the spectrum. The spectra in (b) are from spin echo MRSI data sets obtained from the 50 mM mI/10 mM Cr phantom. Employing a TE of 170 ms with the narrow-bandwidth refocusing pulse minimizes the signal from mI in the region around 3.7 ppm. The TE of 170 ms was chosen after examining spectra acquired with TE varying from 100 to 200 ms; four of these spectra are shown in panel (c) where the variation in mI signal can be observed.

50 mM mI phantom with a small-bandwidth spin echo MRSI sequence with TEs ranging from 100 to 200 ms in steps of 10 ms.

2.1. Data processing and spectral quantification

The *in-vivo* short-TE PRESS spectra were analyzed with LCModel (version 6.1) [25] using the basis set outlined previously [21]. The resultant concentration values were corrected for relaxation by dividing them by $e^{-TE/T_2}(1-e^{-TR/T_1})$. The T_1 and T_2 values for the CH_3 protons of Cr at 3 T were taken to be 1470 ms and 169 ms, respectively [26]. For Glx, T_1 and T_2 values of 1230 ms (averaged over white and gray matter) and 200 ms, respectively, were assumed [27].

For the *in-vivo* TSI data, all spectral reconstruction, processing, and peak fitting was carried out with a Philips automated spectroscopy processing software. Spectra were processed in the range of −1 to 4.4 ppm. The signal decay of the second echo due to T_2 relaxation was corrected for assuming an average T_2 of ≈165 ms for Glx and the CH_2 protons of Cr [26,27]. The data was filtered in the spatial frequency domain with a cosine filter, 2D fast Fourier transformed, filtered in the time domain with a Lorentz–Gauss filter, zero-filled to 512 points, and Fourier transformed to yield a spectrum for each voxel. The spectra were displayed and interpreted in magnitude mode because the abrupt truncation at the beginning of data acquisition led to observable ringing in the real spectra. Baselines were fitted with a fifth degree polynomial and subtracted from the spectra. The resulting spectra were peak fitted with a non-linear least squares iterative method based on the Marquardt and Levenberg algorithm [28,29]. Each peak was represented by a linear combination of a Gaussian and a Lorentzian function. The output of the spectral processing yielded the peak areas and their signal to noise ratios. The noise measurement was propagated to estimate the uncertainties in the Glx peak (≈3.65–≈3.85 ppm) and in the Cr peak (≈3.85–≈4.0 ppm) areas and in their ratio. The 3.9 ppm Cr peak was employed as a reference in this work instead of the 3.0 ppm Cr peak because the latter suffered largely from the chemical shift displacement effect as a result of restricted bandwidth of the refocusing pulses [21]. As with the PRESS spectra, the areas were corrected for relaxation by dividing them by $e^{-TE/T_2}(1-e^{-TR/T_1})$. The T_1 and T_2 values for the CH_2 protons of Cr at 3 T were taken to be 1020 ms and 137 ms, respectively [26], while for Glx the same relaxation time values that were used in correcting the PRESS spectra were assumed. The area of Glx was also doubled to account for the difference in proton multiplicity of the molecular groups contributing to the Cr and Glx resonances. In addition, the Glx area was multiplied by a numerically determined factor of 1.03 to compensate for the small signal loss which results from the strong coupling interactions of the C_3 protons [21].

3. Results and discussion

The left column of Fig. 1 displays the calculated response of the C_2 proton signal of Glu in response to a typical spin echo sequence. The amplitude and phase modulations as a function of TE are a result of the weak scalar coupling that exists between the C_2 and C_3 protons. Such oscillations can lead to spatial misregistration in a TSI sequence [20]. The variations can be eliminated by employing a refocusing pulse that does not excite the C_3 protons in the volume of interest [21]. This is illustrated in the right column of Fig. 1 where the response of the C_2 Glu proton to the modified spin echo sequence is a triplet that remains practically unchanged as TE is altered, and that is therefore rendered suitable for detection by TSI with the only concern being signal decay of successive echoes due to T_2 relaxation.

Results from phantom experiments are shown in Fig. 2. Spin echo spectroscopic imaging sequences were applied to the 50 mM Glu/10 mM Cr phantom and spectra from one of the central voxels are displayed in panel (a). The sequences were applied with the parameters stated in Section 2. The first and second spectra were acquired with spin echo MRSI sequences with refocusing pulse bandwidths of 870 and 175 Hz, respectively. It is clear that employing the small-bandwidth refocusing pulse enhanced the amplitude of the Glu signal by a factor of ≈1.3 [21]. The third spectrum was obtained with a TSI sequence which employed two

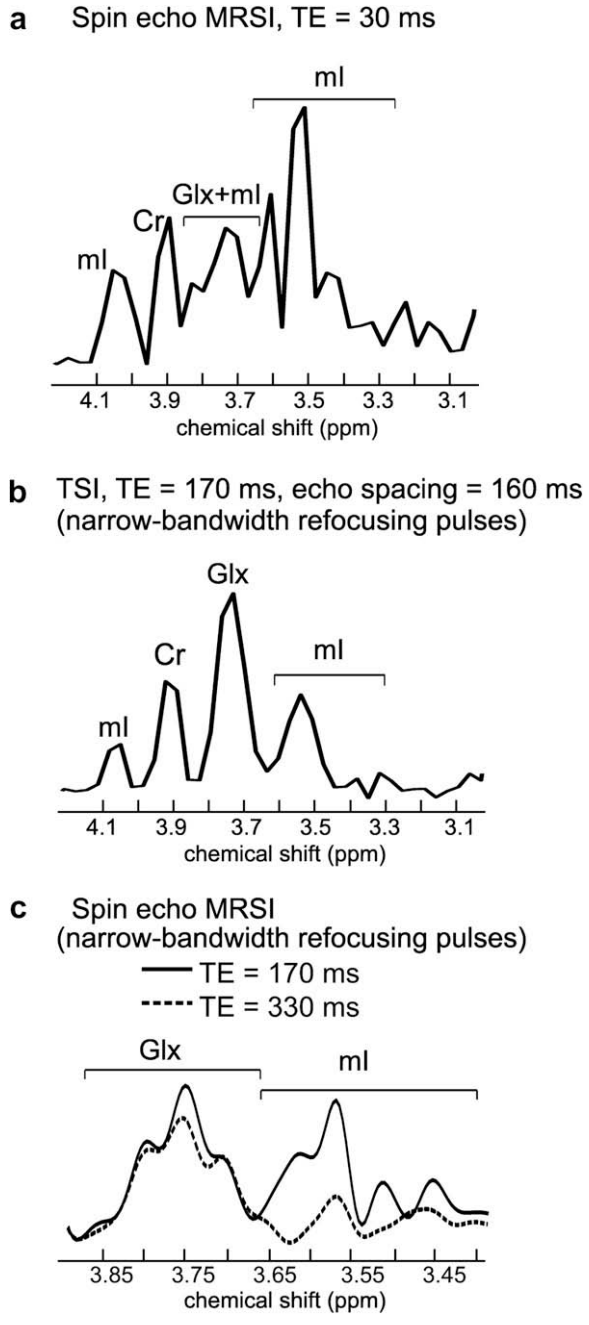

Fig. 3. All spectra are from a central voxel of the 50 mM Glu/24 mM Gln/31 mM mI/10 mM Cr phantom. Spectra (a) and (b) are displayed in magnitude mode. Clearly, with a regular short-TE MRSI sequence, the Glx peak suffers contamination from mI. Exploiting the narrow-bandwidth refocusing pulses and using the optimized TE of 170 ms (echo spacing of 160 ms) results in distinct peaks for Cr, Glx, and mI in approximately half the scan time. Panel (c) displays phase-corrected real spectra of higher spectral resolution (2048 samples), acquired at two different TEs that correspond to the two TSI echoes (170 and 330 ms) with a narrow-bandwidth spin echo MRSI sequence. The Glx spectral pattern remains unchanged with TE.

small-bandwidth refocusing pulses and which read out two echoes per excitation, thus reducing the scan time by a factor of two while yielding spectra of comparable quality. Similar results were obtained for Gln. The spectra in Fig. 2(a) were measured with a TE of 100 ms, the minimum achievable with a readout time of 128 ms. However, it was empirically found that a TE of 100 ms was not optimal for minimizing Glx contamination from mI in the 3.7 ppm spectral region, but rather a TE of 170 ms better served this purpose as is demonstrated in Fig. 2(b). A TE of 170 ms was chosen after examining spectra acquired from the mI phantom with a spin echo MRSI sequence with TEs ranging from 100 to 200 ms; Fig. 2(c) displays four of these spectra and it can be seen that at the selected TE the signal contribution from mI to the Glx spectral region (enclosed by the dashed vertical lines) is minimal. The overlap of mI with Glx is clearly visible in the spectrum of Fig. 3(a) which was obtained from the 50 mM Glu/24 mM Gln/31 mM mI/10 mM Cr phantom with a short-TE spin echo MRSI sequence. In contrast, Fig. 3(b) exhibits the result of applying the limited-bandwidth TSI sequence with the optimized TE of 170 ms; distinct peaks for Cr, Glx, and mI are observed. To more clearly see the spectral patterns that are acquired with each of the TSI echoes, higher resolution spectra were acquired with a narrow-bandwidth spin echo MRSI sequence, first with a TE of 170 ms and then with a TE of 330 ms. A spectrum acquired at each TE from one of the voxels is displayed in Fig. 3(c). Whereas the signal from mI is different at the two echo times because of *J*-coupling evolution, the Glx multiplet maintains its shape and only suffers signal loss due to T_2 relaxation.

The applicability of the sequence *in-vivo* is demonstrated in Figs. 4 and 6. TSI data sets were acquired from three different normal

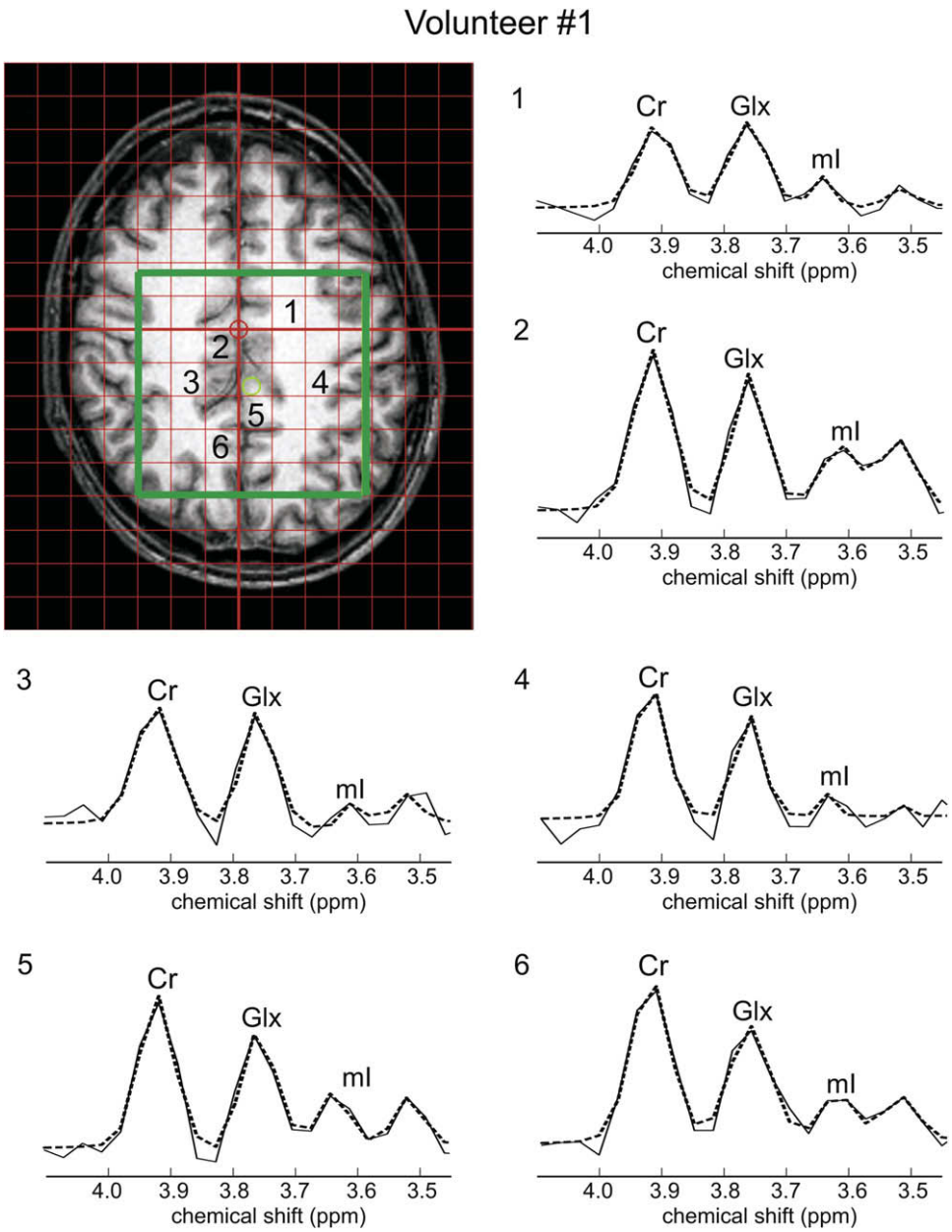

Fig. 4. A TSI sequence (TE = 170 ms, echo spacing = 160 ms) employing refocusing pulses of limited bandwidth was applied to a 15 mm slice that cut through the frontal and parietal lobes of a normal volunteer. Spectra from six selected voxels along with their fitted spectra (dashed lines) are displayed. The spectra are numbered according to their corresponding labelled voxel positions on the image. Each voxel has a nominal volume of $12 \times 12 \times 15$ mm^3. The Glx peaks are clearly visible and are well resolved from Cr and mI.

volunteers from a 15 mm axial slice that cut through the frontal and parietal lobes. A 1 mm T_1 weighted axial slice of one of the volunteers (volunteer #1) is displayed in Fig. 4 with the TSI grid overlaid on it along with the volume of interest on which shimming was performed. Spectra from six of the voxels along with their corresponding fitted spectra (dashed spectra) are displayed. The spectra were processed and fitted according to the procedures described in Section 2.1, and it can be seen that high Glx signal was maintained, the Glx and Cr peaks were well resolved, signal from mI was minimized, and the relatively long TE ensured the decay of the macromolecule baseline. Fig. 5(a) displays the real part of an *in-vivo* TSI spectrum obtained from volunteer #2; the ringing due to the echo discontinuity is visible. The corresponding magnitude mode spectrum along with the fitted baseline is shown in Fig. 5(b), and the result of fitting and baseline subtraction can be seen in Fig. 5(c). The major shortcoming of this method is that the restricted bandwidth of the refocusing pulses limits useful peaks for the purposes of quantification to those of Glx (≈3.75 ppm) and Cr (≈3.9 ppm). The other peaks experience the refocusing pulses in slices that are significantly shifted from the target slice. Therefore, the Cho (≈3.2 ppm) and Cr (≈3 ppm) peaks visible in the spectra of Fig. 5 represent signal from a portion of the slice of interest, preventing the Cr peak at 3 ppm from serving the purpose of an internal concentration reference as it often does [30,31], leaving the Cr peak at 3.9 ppm to play this role instead. Shifting the frequency of the refocusing pulse towards 3 ppm would maintain more of the Cr peak at 3 ppm but at the expense of reducing the target Glx signal. It is also apparent that there is no trace of NAA around 2 ppm because spins in this spectral region experience the refocusing pulse in a slice that does not overlap with the target slice. Another drawback is that because the glutamate moiety of glutathione (GSH) exhibits significantly similar chemical shift and scalar coupling properties to those of Glu and of Gln [32], the *J*-coupling evolution of the GSH proton at ≈3.77 ppm will also be rewound by the presented method thus contaminating the Glx peak by an amount proportional to its concentration. Based on the Glu, Gln, and GSH concentrations listed in Ref. [24], and the chemical shift and scalar coupling values stated in Ref. [32] it was simulated that ≈14% of the Glx peak could be attributed to GSH.

Although quantification was not the main purpose of this work, we attempted to quantify the relative concentration of Glx to Cr from TSI data obtained from volunteers #2 and #3. Spectra from two of the TSI voxels (containing a mixture of gray and white matter) were summed for each volunteer from the regions displayed in Fig. 6 and corresponding short-TE PRESS spectra from those volumes were also acquired. Fig. 6 shows the summed TSI spectrum and the corresponding PRESS spectrum for each of the two cases. LCModel was employed to analyze the short-TE spectra and the output was compared to concentration ratios that were deduced from the corresponding TSI spectra (see Section 2.1 for analysis details). The results are summarized in Table 1 with the volunteer numbering corresponding to that of Fig. 6. In each case, the ratios determined from the TSI spectra are ≈13% lower than the ratios provided by LCModel analysis; however, both sets of ratios do agree within error which indicates the feasibility of measuring Glx levels relative to Cr with the method presented in this work. The technique particularly lends itself to monitoring Glx to Cr ratios in longitudinal MRS studies.

The presented method is not limited to Glx detection but can be applied to any weakly coupled proton spin system. For example, it would be suitable for targeting the CH_3 protons of Lac (lactate) which resonate around 1.3 ppm. Lactate, to our knowledge, is the only metabolite with a coupled spin system that has previously been detected by TSI. This was achieved by setting the echo time and the echo spacing to multiples of $1/J$, where J is the scalar coupling constant between the 1.3 ppm Lac protons and the 4.1 ppm proton, and reversing the sign of all the odd echoes [20,33]. The technique described in this work would allow Lac observation by TSI without placing any restrictions on the echo time and the echo spacing, and without requiring sign reversals of any of the echoes. Furthermore, it would avoid the downsides associated with Lac detection at higher field strengths, such as 3 T, where the chemical shift difference between the weakly coupled Lac protons becomes comparable to the bandwidths of the RF pulses [34,35].

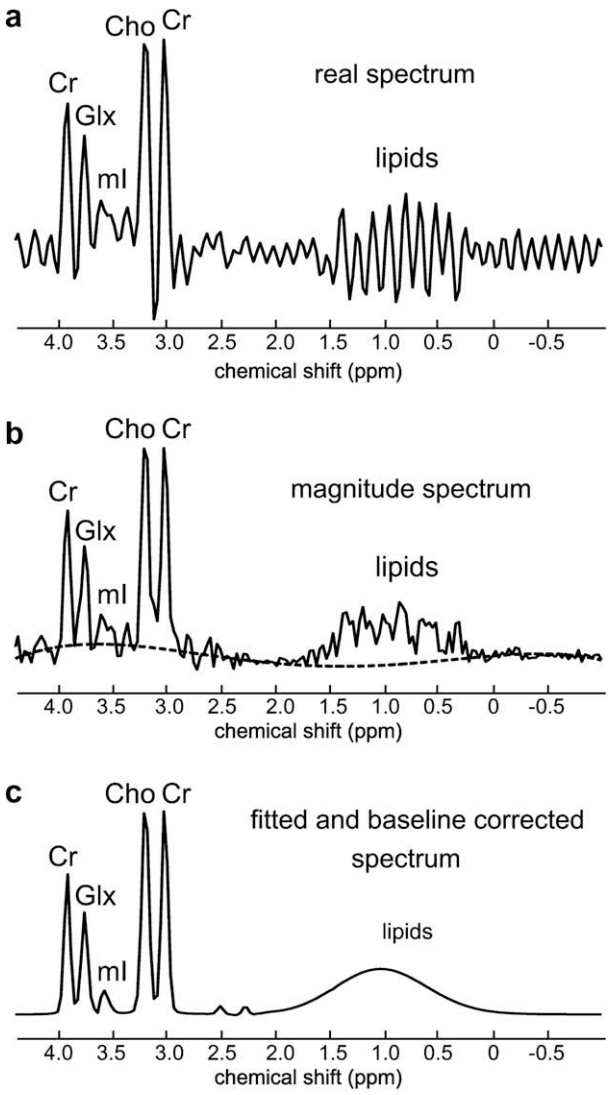

Fig. 5. Spectrum (a) demonstrates the ringing due to the echo discontinuity in the real part of an *in-vivo* TSI spectrum obtained from volunteer #2. The magnitude of the spectrum along with the fitted baseline (dashed curve) is displayed in (b). The result of fitting and baseline subtraction can be seen in (c).

The technique, however, cannot rewind the scalar coupling evolution of protons that are engaged in both weak and strong coupling interactions because of the complex coherence proliferation of strongly coupled spins [36]. Therefore, the method is not applicable, for example, to the C_3 protons of Glu or to the mI protons that resonate in the vicinity of ≈3.55 ppm. Nevertheless, the sequence could be tailored for observing the mI proton resonating at ≈4.06 ppm, which, like the C_2 proton of Glu, is solely involved in weak coupling. However, at 3 T, this would require a refocusing pulse of bandwidth less than approximately 66 Hz (the chemical shift difference between the 4.06 mI proton and the protons to which it is weakly coupled).

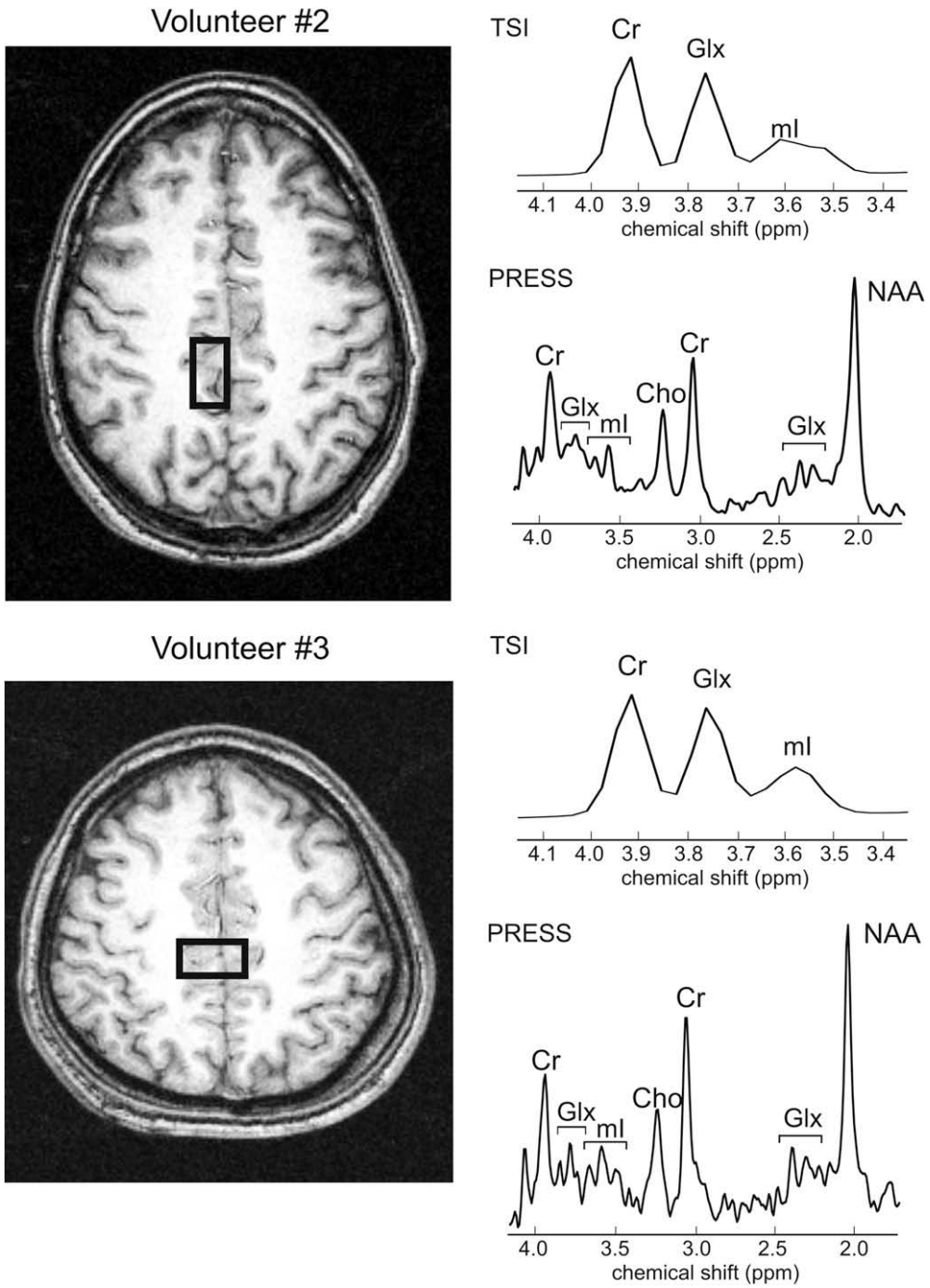

Fig. 6. The TSI sequence that was applied to volunteer #1 was also applied to volunteers #2 and #3. To assess the feasibility of Glx quantification from the TSI spectra, a short-TE (TE = 35 ms) single voxel PRESS spectrum was also acquired from each volunteer from the regions indicated on the images. These regions were chosen such that they overlapped with two of the TSI voxels. For each volunteer, the spectra from the two voxels were summed. The summed TSI spectra along with their corresponding PRESS spectra are shown.

Table 1
Summary of concentration ratios obtained from the short-TE PRESS spectra (LCModel analysis) and from the corresponding summed TSI spectra (integration of fitted peaks). The volunteer numbering is consistent with Fig. 6, where the spectra are displayed.

Volunteer #	[Glx]/[Cr] by LCModel analysis of short-TE spectrum	[Glx]/[Cr] by fitting and integrating of TSI spectrum
2	1.57 ± 0.22	1.38 ± 0.23
3	1.43 ± 0.21	1.23 ± 0.18

4. Conclusion

In this paper, we demonstrated a method that facilitates the detection of the C_2 protons of Glx by TSI. The resulting spectra exhibited a Glx peak of high signal that was well resolved from Cr and mI. The approach is also applicable to other spin systems whose scalar coupling interactions are limited to the weak-coupling regime, and it involves utilizing TSI refocusing pulses that have bandwidths less than the chemical shift difference between the target spins and the spins to which they are weakly coupled.

This permits rewinding of the *J*-evolution of the target protons in the slice of interest regardless of the selected echo time and echo spacing. Thus constant signal is provided from echo to echo rendering weakly coupled spins as potential candidates for measurement by the time efficient TSI sequence.

Acknowledgments

We appreciate the financial support of the Canadian Foundation for Innovation (CFI) and the Alberta Science and Research Investment Program (ASRIP). We acknowledge Philips Medical Systems for research support. We also wish to thank Dr. Burkhard Mädler for assistance with the LCModel analysis and Dr. Ulrike Dydak for a helpful discussion.

References

[1] Y.D. Cho, G.H. Choi, S.P. Lee, J.K. Kim, ^{1}H-MRS metabolic patterns for distinguishing between meningiomas and other brain tumors, Magn. Reson. Imaging 21 (2003) 663–672.
[2] G. Hasler, J.W. van der Veen, T. Tumonis, Reduced prefrontal glutamate/glutamine and gamma-aminobutyric acid levels in major depression determined using proton magnetic resonance spectroscopy, Arch. Gen. Psychiatry 64 (2007) 193–200.
[3] N. Hattori, K. Abe, S. Sakoda, T. Sawada, Proton MR spectroscopic study at 3 Tesla on glutamate/glutamine in Alzheimer's disease, Neurochemistry 13 (2002) 183–186.
[4] G. Helms, Volume correction for Edema in single-volume proton MR spectroscopy of contrast-enhancing multiple sclerosis lesions, Magn. Reson. Med. 46 (2001) 256–263.
[5] M. Rijpkema, J. Schuuring, Y. van der Meulen, M. van der Graaf, H. Bernsen, R. Boerman, A. van der Kogel, A. Heerschap, Characterization of oligodendrogliomas using short echo time ^{1}H MR spectroscopic imaging, NMR Biomed. 16 (2003) 12–18.
[6] I. Savic, A.M. Thomas, Y. Ke, J. Curran, I. Fried, J. Engel, *In vivo* measurements of glutamine + glutamate (Glx) and *N*-acetyl aspartate (NAA) levels in human partial epilepsy, Acta Neurol. Scand. 102 (2000) 179–188.
[7] J. Frahm, K.-D. Merboldt, W. Hanicke, J. Magn. Reson. 72 (1987) 502–508.
[8] P.A. Bottomley, Selective volume method for performing localized NMR spectroscopy, US Patent 4,480,228, 1984.
[9] D.T. Chard, M.A. McLean, G.J.M. Parker, D.G. MacManus, D.H. Miller, Reproducibility of in vivo metabolite quantification with proton magnetic resonance spectroscopic imaging, J. Magn. Reson. Imaging 15 (2002) 219–225.
[10] J. Sastre-Garriga, G.T. Ingle, D.T. Chard, L. Ramió-Torrentà, M.A. McLean, D.H. Miller, A.J. Thompson, Metabolite changes in normal-appearing gray and white matter are linked with disability in early primary progressive multiple sclerosis, Arch. Neurol. 62 (2005) 569–573.
[11] R.J. Simister, F.G. Woermann, M.A. McLean, P.A. Bartlett, G.J. Barker, J.S. Duncan, A short-echo-time proton magnetic resonance spectroscopic imaging study of temporal lobe epilepsy, Epilepsia 43 (2002) 1021–1031.
[12] J.H. Duyn, J. Gillen, G. Sobering, P.C.M. Van Zijl, C.T.W. Moonen, Multisection proton MR spectroscopic imaging of the brain, Radiology 188 (1993) 277–282.
[13] T.J. DeVito, D.J. Drost, R.W.J. Neufeld, N. Rajakumar, W. Pavlosky, P. Williamson, R. Nicolson, Evidence for cortical dysfunction in autism: a proton magnetic resonance spectroscopic imaging study, Biol. Psychiatry 61 (2007) 465–473.
[14] P.B. Barker, D.D.M. Lin, In vivo proton MR spectroscopy of the human brain, Prog. Nucl. Magn. Res. Sp. 49 (2006) 99–128.
[15] J.H. Duyn, C.T.W. Moonen, Fast proton spectroscopic imaging of human brain using multiple spin-echoes, Magn. Reson. Med. 30 (1993) 409–414.
[16] U. Dydak, D. Meier, R. Lamerichs, P. Boesiger, Trading spectral separation at 3 T for acquisition speed in multi spin-echo spectroscopic imaging, Am. J. Neuroradiol. 27 (2006) 1441–1446.
[17] W. Block, F. Jessen, F. Träber, S. Flacke, C. Manka, R. Lamerichs, E. Keller, R. Heun, H. Schild, Regional *N*-acetyl aspartate reduction in the hippocampus detected with fast proton magnetic resonance spectroscopic imaging in patients with Alzheimer disease, Arch. Neurol. 59 (2002) 828–834.
[18] S. Flacke, F. Träber, W. Block, R. Lamerichs, H. Schüller, H.H. Schild, Improved diagnosis of contrast-enhancing brain lesions with multifunctional MRI assessment: a case report, J. Magn. Reson. Imaging 9 (1999) 741–744.
[19] A.J. Martin, H. Liu, W.A. Hall, C.L. Truwit, Preliminary assessment of turbo spectroscopic imaging for targeting in brain biopsy, Am. J. Neuroradiol. 22 (2001) 959–968.
[20] R.V. Mulkern, H. Chao, J.L. Bowers, D. Holtzman, Multiecho approaches to spectroscopic imaging of the brain, Ann. NY Acad. Sci. 820 (1997) 97–122.
[21] A. Yahya, B. Mädler, B.G. Fallone, Exploiting the chemical shift displacement effect in the detection of glutamate and glutamine (Glx) with PRESS, J. Magn. Reson. 191 (2008) 120–127.
[22] J. Shen, R.E. Rycyna, D.L. Rothman, Improvements on an in vivo automatic shimming method (FASTERMAP), Magn. Reson. Med. 38 (1997) 834–839.
[23] A. Haase, J. Frahm, W. Hanicke, D. Matthaei, ^{1}H NMR chemical shift selective (CHESS) imaging, Phys. Med. Biol. 30 (1985) 341–344.
[24] R.A. De Graaf, D.L. Rothman, *In vivo* detection and quantification of scalar coupled ^{1}H NMR resonances, Concepts Magn. Reson. 13 (2001) 32–76.
[25] S.W. Provencher, Estimation of metabolite concentrations from localized *in vivo* proton NMR spectra, Magn. Reson. Med. 30 (1993) 672–679.
[26] F. Träber, W. Block, R. Lamerichs, J. Gieseke, H.H. Schild, ^{1}H metabolite relaxation times at 3.0 Tesla: measurements of T_1 and T_2 values in normal brain and determination of regional differences in transverse relaxation, J. Magn. Reson. Imaging 19 (2004) 537–545.
[27] S. Posse, R. Otazo, A. Caprihan, J. Bustillo, H. Chen, P.-G. Henry, M. Marjanska, C. Gasparovic, C. Zuo, V. Magnotta, B. Mueller, P. Mullins, P. Renshaw, K. Ugurbil, K.O. Lim, J.R. Alger, Proton echo-planar spectroscopic imaging of *J*-coupled resonances in human brain at 3 and 4 Tesla, Magn. Reson. Med. 58 (2007) 236–244.
[28] K. Levenberg, A method for the solution of certain problems in least squares, Quart. Appl. Math. 2 (1944) 164–168.
[29] D. Marquardt, An algorithm for least-squares estimation of nonlinear parameters, SIAM J. Appl. Math. 11 (1963) 431–441.
[30] C. Choi, N.J. Coupland, P.P. Bhardwaj, N. Malykhin, D. Gheorghiu, P.S. Allen, Measurement of brain glutamate and glutamine by spectrally-selective refocusing at 3 Tesla, Magn. Reson. Med. 55 (2006) 997–1005.
[31] I.-Y. Choi, S.-P. Lee, H. Merkle, J. Shen, Single-shot two-echo technique for simultaneous measurement of GABA and creatine in the human brain in vivo, Magn. Reson. Med. 51 (2004) 1115–1121.
[32] V. Govindaraju, K. Young, A.A. Maudsley, Proton NMR chemical shifts and coupling constants for brain metabolites, NMR Biomed. 13 (2000) 129–153.
[33] J.H. Duyn, J.A. Frank, C.T.W. Moonen, Incorporation of lactate measurement in multi-spin-echo proton spectroscopic imaging, Magn. Reson. Med. 33 (1995) 101–107.
[34] T. Lange, U. Dydak, T.P.L. Roberts, H.A. Rowley, M. Bjeljac, P. Boesiger, Pitfalls in lactate measurements at 3 T, Am. J. Neuroradiol. 27 (2006) 895–901.
[35] D.A. Yablonskiy, J.J. Neil, M.E. Raichle, J.J.H. Ackerman, Homonuclear J coupling effects in volume localized NMR spectroscopy: pitfalls and solutions, Magn. Reson. Med. 39 (1998) 169–178.
[36] L.E. Kay, R.E.D. McClung, A product operator description of AB and ABX spin systems, J. Magn. Reson. 77 (1988) 258–273.